

## AN INVESTIGATION OF THE DIXIE VALLEY GEOTHERMAL FIELD, NEVADA, USING TEMPORAL MOMENT ANALYSIS OF TRACER TESTS

Marshall J. Reed

U. S. Geological Survey, MS-977  
345 Middlefield Road  
Menlo Park, CA 94025, USA  
mjreed@usgs.gov

### ABSTRACT

The method of analysis of the first temporal moment (mean residence time) of tracer return data was utilized to investigate the swept volume and fluid velocity between pairs of injection and production wells in the Dixie Valley geothermal field. Calculations were made using a spreadsheet program available from the Idaho National Laboratory. Jointly sponsored industry-government research at the Dixie Valley field provided several tracer tests over many years, and a test of six, chemically similar tracers, injected between 1998 and 2001, provided the tracer concentration data used in this study. The calculated parameters of mean residence time, fracture volume in contact with the tracer, fluid velocity, and heterogeneity of the reservoir were compared to published descriptions of the reservoir to evaluate their usefulness in refining the conceptual model of the Dixie Valley geothermal reservoir. Temporal moment analysis provided more information about the fractured fluid path between wells and the volume of the reservoir contacted by the tracers. Tracer injection in the center of the Dixie Valley field and production of that tracer in the northeastern and southwestern production wells clearly demonstrated that no barrier to flow exists between the two areas of producing wells.

### INTRODUCTION

The Dixie Valley geothermal field in north-central Nevada (Figure 1) is confined to narrow fractures developed along permeable, southeast-dipping zones of the Stillwater Fault on the western margin of Dixie Valley (Benoit, 1992). The undisturbed reservoir fluid was a bicarbonate-chloride type water at a temperature of 250°C (Reed, 1989), but subsequent injection of brine from the steam separators has increased the chloride and decreased the bicarbonate concentrations. The Dixie Valley power plant provides 62 MW gross electrical generation that requires  $2.1 \cdot 10^6$  kg/h of fluid production from the geothermal wells (Desormier, 1987). Continuous operation of the power plant began in July 1988, and

the fluid injection system began operation in September 1988 (Benoit, 1992). Early injection was unable to keep up with the withdrawal of reservoir water, and, by the end of 1998, power plant operations and well testing resulted in the loss, through evaporation and surface discharge, of  $6.95 \cdot 10^{10}$  kg of fluid from the single-phase liquid, geothermal reservoir (Benoit et al., 2000). The decline in reservoir pressure prompted the drilling of five additional production wells to maintain the energy input to the power plant, but the subsequent decline in production from the new wells indicated the need for injection augmentation with fluid from a shallow water well (Benoit et al., 2000). A well for injection augmentation (Figure 1), the Goerenger shallow water well, provided injection water at pumped rates up to 133 L/s (Benoit et al., 2000).

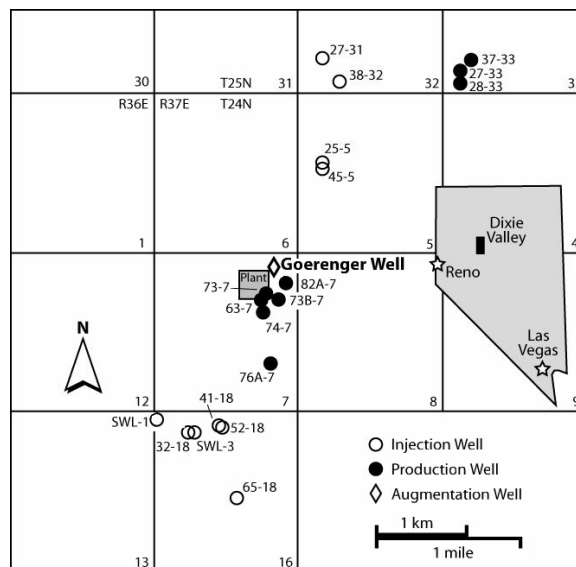


Figure 1. Dixie Valley Location Map. Surface locations for production and injection wells in the Dixie Valley geothermal field (modified from Benoit et al., 2000).

Water injection is critical to the operation of all geothermal fields in order to maintain reservoir pressure and to sustain well productivity, and the injection wells in Dixie Valley were chosen to disperse the injected fluid in several geologic environments primarily to maintain reservoir pressure and secondarily to minimize reservoir cooling (Benoit, 1992). Three wells (SWL-1, SWL-3, 32-18) inject fluid into a sub-horizontal, lower temperature (220°C) aquifer in Miocene basalts east of the range-front fault at depths between 2192 m and 2248 m; three wells (41-18, 52-18, 65-18) inject fluid into deep, lower temperature (225° to 230°C) zones of the range-front fault between depths of 2713 m and 2815 m; and two wells (25-5, 45-5) inject fluid into shallow, lower temperature (205°C) zones in a Miocene basalt on the range-front fault at depths between 1776 m and 1876 m (Benoit, 1992). Two more recent wells (27-32, 38-32) have only been used for injection of cold steam condensate and augmentation water into a shallow (180 m deep) fault zone which was originally an outflow plume from the reservoir (Rose et al., 2001; T. DeRocher, personal communication, 2007).

The effective flow path of fluid through a geothermal reservoir can be determined by the injection of chemical tracers and the detection of those tracers in the flow from production wells. Tracer testing can also give an indication of when the cold front in the reservoir fluid will intersect a producing well (Shook, 2001). The ideal tracer is soluble in the geothermal fluid, is stable at reservoir temperatures, does not adsorb or react with the reservoir rocks, can be detected at low concentrations, and does not damage the environment. For many years, the Geothermal Technologies Program of the U. S. Department of Energy has funded research for the identification and testing of chemicals that can be used as geothermal tracers and for tracer-test analysis and interpretation. As part of the joint industry-government geothermal research in the Dixie Valley geothermal field, testing of potential chemical tracers has been conducted over several years.

One of the research projects involved the introduction of six distinctive naphthalene-sulfonate compounds as liquid-phase tracers into six different injection wells at Dixie Valley. Two tracer tests were initiated in each of the years 1998, 1999, and 2001, and the sampling and analysis of tracer concentrations continued to May 2004 (Rose et al., 2000, 2001, and 2002). Tracer analysis used a combination of liquid chromatography and ultraviolet-fluorescence spectroscopy to detect very low concentrations of the naphthalene sulfonate compounds, and the detection limit estimated for the first two naphthalene sulfonates was approximately 200 parts per trillion by volume (200 pL/L). The thermal stabilities of these two tracers were reported as half-lives over 400 days

for temperatures above 275°C (Rose et al., 2001). During the period of the six tracer tests, July 1998 to May 2004, ten different wells were in use as fluid injectors, and nine wells were in use for production of hot water and steam for the power plant (Figure 1).

The liquid injected into the reservoir consisted of a mixture of hot water (110°C) separated from the steam supplied to the power plant, cooling tower overflow (steam condensate, 40°C), and shallow ground water (25°C) for augmentation (Benoit et al., 2000). A special pipeline was used to transport only a mixture of steam condensate and augmentation water for injection into wells 27-32 and 38-32 (T. DeRocher, personal communication, 2007). The daily flow rates for each well were provided by the Caithness Operating Company, LLC (Caithness proprietary data, 2006). The flow rate of each well varied considerably over the period of the tracer tests due to changes in field operations and periods of well maintenance. During the time of the tracer testing, the entire field was shut down twice for power plant inspection and maintenance: October 3, 1998 for 14 days and October 4, 2003 for 17 days.

In order to simplify the analysis of tracer testing, G. M. Shook and J. H. Forsmann (2005) developed a spreadsheet program to calculate the first temporal moment (equal to the mean residence time) of tracer return data and to investigate the swept volume and fluid velocity between pairs of injection and production wells (described by Shook, 2003). Nomenclature and symbols used in this report are from Shook and Forsmann (2005). This method was previously used to analyze tracer test data from the Beowawe geothermal field, Nevada (Shook, 2005). The contribution presented here utilizes the spreadsheet analysis of the first temporal moment from tracer-test data to characterize the reservoir in the Dixie Valley geothermal field and to help refine the conceptual model of the geothermal reservoir.

## **TRACER TEST OPERATIONS**

P. E. Rose provided the data set for the tracer testing at Dixie Valley (Rose, personal communication, 2005). This data set contained the date and mass of the initial tracer injection, the dates of fluid sample collection from production wells, and the tracer concentrations (in nL/L) from analyses of produced fluid. This group of tracer tests was initiated on July 14, 1998, with a mass of 100 kg of 1,5-naphthalene disulfonate (1,5-NDS) injected into well 41-18 and a mass of 100 kg of 1,3,6-naphthalene trisulfonate (1,3,6-NTS) injected into well 65-18 (Rose et al., 2000). These and subsequent tracers were injected quickly (the entire mass of tracer was injected in less than 30 minutes). This type of rapid tracer injection, called a slug injection, is required for the calculation of the first temporal moment (Shook, 2005). On

November 17, 1999, a mass of 200 kg of 2,7-naphthalene disulfonate (2,7-NDS) was injected into well 27-32, and on November 18, 1999, a mass of 200 kg of 2-naphthalene sulfonate (2-NS) was injected into well 25-5 (Rose et al., 2001). The last two tracers were injected on July 10, 2001, with a mass of 143 kg of 1-naphthalene sulfonate (1-NS) injected into well 45-5 and a mass of 150 kg of 2,6-naphthalene disulfonate (2,6-NDS) injected into well 38-32 (Rose et al., 2002). The sampling and analysis for all six tracers continued through May 6, 2004 (2,123 days after injection of the first pair of tracers). The time interval between sample collections of produced fluid for tracer analysis varied from two days to more than 125 days.

In the discussion of injection of 2-NS into well 25-5 (Rose et al., 2001), the authors draw attention to a significant background concentration between 2 and 3.8 nL/L of a compound that was indistinguishable from the tracer. This type of background contamination could be due to isomerization or partial decomposition of any of the naphthalene sulfonate tracers or related polyaromatic sulfonate tracers injected into the reservoir in earlier tracer tests (Rose et al., 2001). The data set used for this current report had corrected tracer concentrations, in which the background levels in the tracer analyses had been subtracted. The tracer volume concentrations were converted to mass concentrations with the application of the average density of 0.995 kg/L for the production samples (Rose, personal communication, 2006).

### **TRACER TEST INTERPRETATION**

Use of the spreadsheet to calculate temporal moments (Shook and Forsmann, 2005) required three assumptions: (1) the tracer should be highly soluble in only one phase of the reservoir fluid, (2) the tracer must be stable, and (3) the flow for injection and production should have reached a steady state. The solubility of the tracers in the liquid phase and the tracer stability have been discussed (Rose et al., 2001). The assumption of steady state flow requires further consideration.

Field operations caused considerable variation in the daily flow rate of each well during the period of the tracer tests, and these conditions violate the strict assumption of steady state flow. Nevertheless, tracer production curves for some wells indicate that in this complex, multi-well field tracer flow through the reservoir may exhibit less variability than the changes in flow rates of individual wells. For example, the plots of 2-NS tracer recovery for each of the wells 63-7, 73-7, and 73B-7 in the close grouping near the power plant are remarkably similar over the same time period (Figure 2). Even though well 73-7 was shut-in for the first part of the tracer test, the first

sample (on day 296) and subsequent samples from well 73-7 closely follow the decline in tracer recovery shown by wells 63-7 and 73B-7. Comparison of the plots of tracer recovery for the three wells indicates that they were all responding to the same tracer concentration in the reservoir segment providing fluid to the wells. Examination of tracer returns from these three wells shows that the direction and velocity of tracer flow through the reservoir was established independently of variations in the production rate of well 73-7. There is value to the calculation of moment analysis to understand the injection-production well pairs even though the variable flow rates of the production wells violate the assumption of steady state flow.

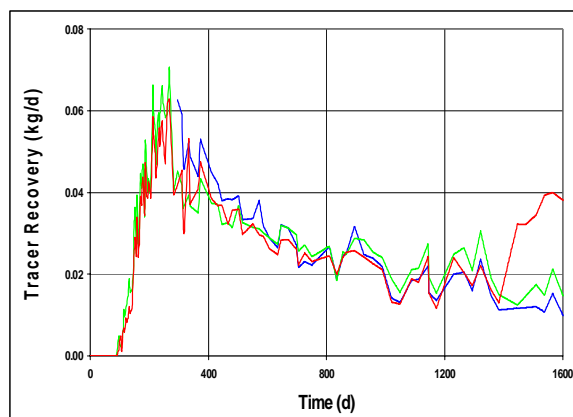


*Figure 2. Graph of Tracer Recovery versus Time. Recovery of tracer in kg/d from wells 73-7 (blue), 73B-7 (green), and 63-7 (red) resulting from tracer injection into well 25-5. The tracer recovery plots show great similarity between wells.*

Several steps were taken to smooth the tracer recovery data to more closely approximate steady state flow. The tracer records of the production and injection wells were compressed to eliminate the two extended periods when the field was shut down for power plant maintenance. Each value of mass concentration for the samples of produced tracer was multiplied by the well flow rate of the production well on the day of sample collection to obtain the mass of tracer produced, and the tracer recovery for each day between sample collections was determined by straight-line interpolation. The mass of tracer produced was then normalized by dividing by the mass of initial tracer injection (slug injection) to obtain  $E_{app}(t)$ , the apparent age distribution function of the tracer (with dimension of  $day^{-1}$ ), used by Shook (2005). This interpolation between tracer samples produced a smoothed function that eliminated much of the daily variability in well flow rate. The age distribution function for reinjection of produced tracer,  $E_{in}(t)$ , was calculated for each injection well by multiplying the sum of the daily tracer production,  $E_{app}(t)$ , by the proportion of the

daily flow rate of each injection well to the total mass flow of injection.  $E_{in}(t)$  of the injected tracer was delayed by one day from  $E_{app}(t)$  of the produced tracer to account for the travel time of the fluid from the production wells to the injection wells. Since the naphthalene sulfonate tracers were only soluble in the liquid phase and did not carry over to the separated steam or the steam condensate, the injection wells 27-32 and 38-32 have never injected any recycled tracer (T. DeRocher, personal communication, 2007).

Tracer reinjection creates tracer production histories that are the combined response to the initial slug injection of tracer and the continuous recycling of the produced tracer (Shook, 2005). The spreadsheet calculation takes the combined response of the apparent age distribution function,  $E_{app}(t)$ , of the tracer produced and uses the age distribution function,  $E_{in}(t)$ , of the reinjected tracer to deconvolve the combined response of the production history (Shook and Forsmann, 2005). Moment analysis is based solely on the response to the initial slug of tracer injection (Shook, 2005), so the spreadsheet produces a corrected mass function,  $E_{corr}(t)$ , for the production well by removing the effect of tracer recycling (Figure 3).

The user of the moment analysis spreadsheet is required to examine each tracer history to find a portion of the tracer decline curve that could be fitted to a semi-log straight line. Only sixteen pairs of injection and production wells provided tracer histories with a clear peak and later decline curve that could be fitted to a semi-log straight line, conditions which were needed for the analysis of the first temporal moment. In some unusable tracer histories, production wells exhibited a continuing increase in tracer recovery (Figure 4), and, in other histories, production wells failed to show a clear peak and the following decline in tracer recovery (Figure 5). These problematic records of tracer recovery could not be interpreted for the first temporal moment. For those wells demonstrating a clear peak and semi-log straight segment of the tracer decline, the tracer production was extrapolated to late time with an exponential decline function (Figure 6), and spreadsheet interpretation provided the first temporal moment (mean residence time) and pore volume (fracture volume in contact with the tracer). Several of the tracer histories from producing wells show multiple peaks of tracer recovery (Figure 7). These separate peaks are consistent with the interpretation that fluid flow through the reservoir is within several isolated, sub-parallel fractures of different lengths or permeabilities that require different periods of time to deliver the tracer to the production well.

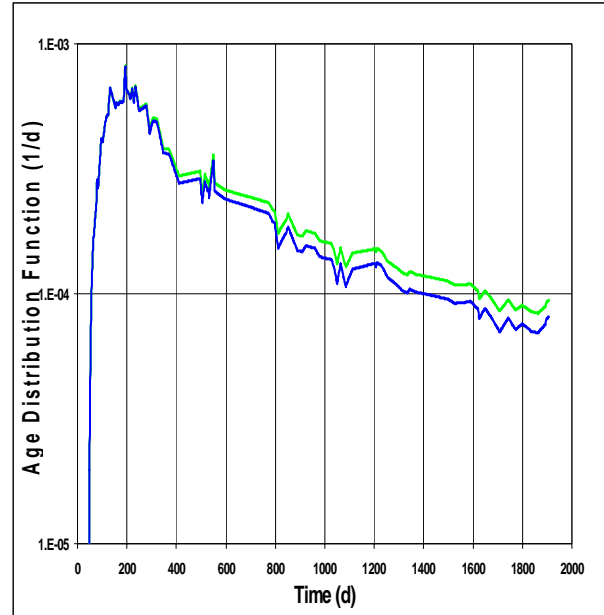


Figure 3. Graph of the Deconvolved Tracer Distribution Function versus Time  
The corrected age distribution function,  $E_{corr}(t)$  [blue], is derived from the apparent age distribution function,  $E_{app}(t)$  [green], by deconvolving the recycled tracer,  $E_{in}(t)$ . Data represent injection of tracer into well 41-18 and production of tracer from well 76A-7.

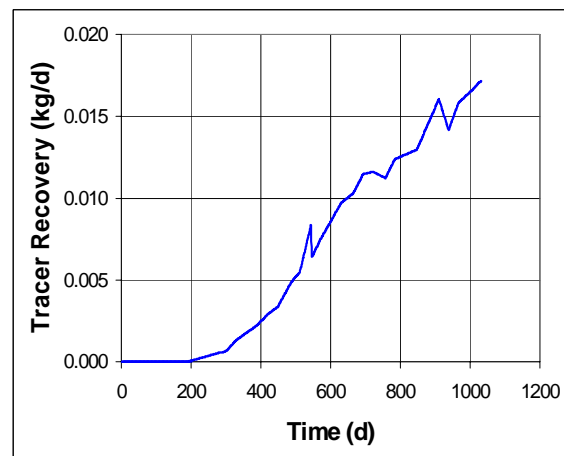


Figure 4. Graph of Tracer Recovery versus Time  
Continued increase of tracer recovery with time is demonstrated by production well 74-7 from injection of tracer into well 38-32.

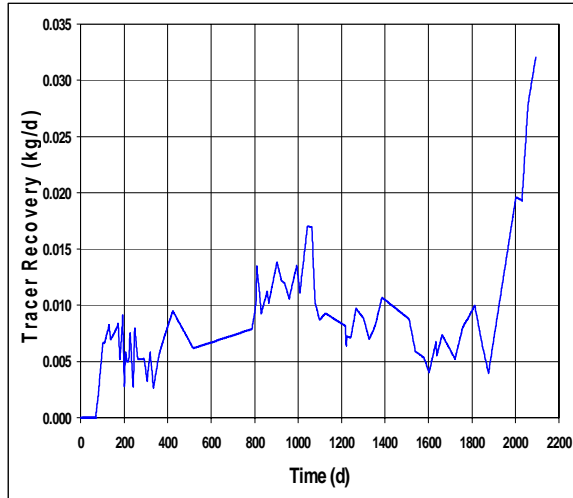


Figure 5. Graph of Tracer Recovery without a Clear Peak  
Tracer Recovery from well 73-7 in response to injection into well 65-18 shows no clear peak and has an anomalous increase in tracer at late time.

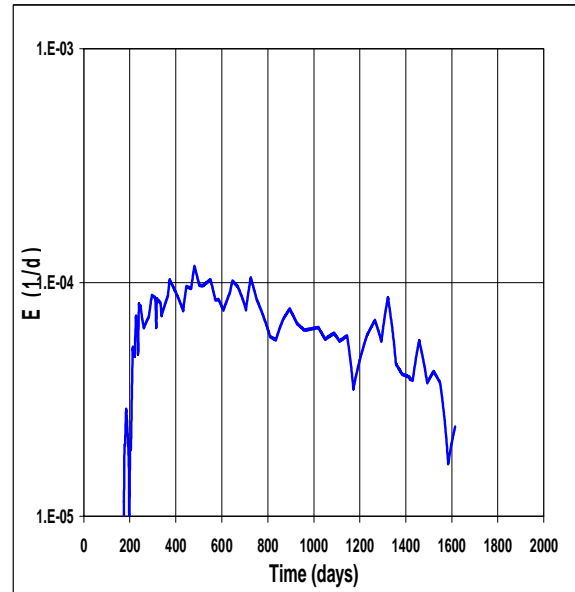


Figure 7. Graph of Tracer Distribution Function with Multiple Peaks  
This corrected age distribution function demonstrates multiple tracer peaks which are interpreted to represent tracer flow through several isolated fractures. Tracer was injected into well 25-5, and production of tracer was from well 76A-7.

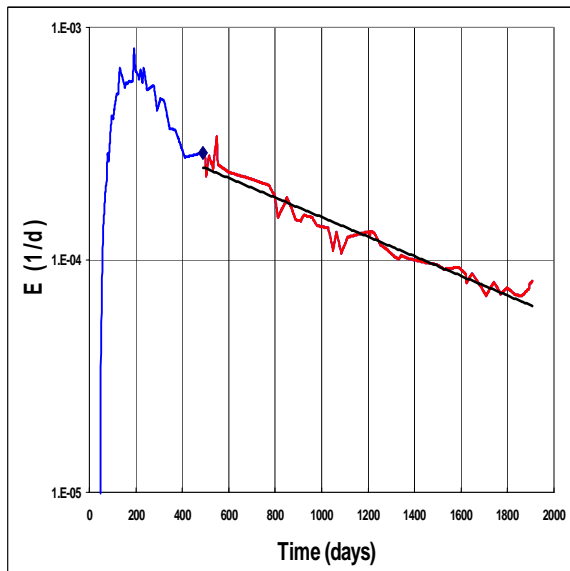


Figure 6. Graph of Exponential Decline Fit to Semi-log Plot  
This semi-log plot of  $E_{corr}(t)$  for tracer production from well 76A-7 in response to injection into well 41-18 demonstrates a linear portion (pink) of the tracer decline and the exponential function (black) for extrapolation to late time.

Individual flow paths are imagined as streamlines with unique values of permeability, porosity, cross sectional area, and length (Shook and Forsmann, 2005). However, the streamline characteristics are independent of the exact formation properties (Shook, 2005). The spreadsheet calculates the flow capacity of the individual streamline as its specific velocity relative to the bulk velocity, and the storage capacity is the pore volume associated with that streamline (Shook, 2005). The spreadsheet also plots the  $F-\Phi$  curve (Figure 8) showing the flow capacity versus the storage capacity (Shook and Forsmann, 2005). At any point on the  $F-\Phi$  plot, the cumulative flow capacity,  $F$ , is the sum of all streamlines whose velocity is greater than the velocity at that chosen point, and the cumulative storage capacity,  $\Phi$ , of those streamlines is the sum of their individual pore volumes (Shook and Forsmann, 2005).

## RESULTS

The flow of tracer from injection well to production well is the sum of flows through individual fractures, and the flow between each pair of wells can be considered as a set of stream-lines that does not interfere with the other sets of stream lines in the field (Shook, personal communication, 2006). The sum of all sets of stream-lines, the entire volume of fractures carrying tracer for all well pairs, is the total

volume of the tested reservoir (Shook and Forsmann, 2005).

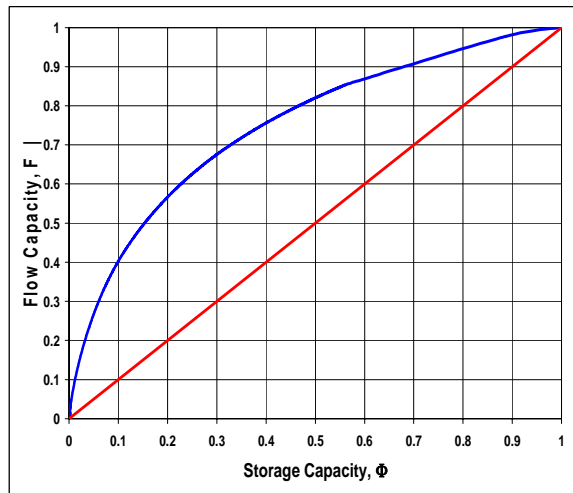


Figure 8. Graph of the Flow Capacity versus the Storage Capacity

The plot of the  $F-\Phi$  curve (blue) shows the heterogeneity in the flow system between injection well 41-18 and production well 76A-7. The point on the  $F-\Phi$  curve at  $\Phi=0.1$  and  $F=0.4$  indicates that 10% of the pore volume (fracture volume) provides 40% of the fluid flow, or, stated differently, a small number of fractures provide a large amount of the fluid flow. The diagonal line (red) represents a reference of homogeneous flow with equal increments of pore volume providing equal amounts of fluid flow.

Based on incomplete tracer returns in earlier testing, researchers working in the Dixie Valley field proposed a barrier between the section seven production wells and the section 33 production wells (Rose, personal communication, 2006). In this analysis of the tracer tests, the production wells in section 33 (wells 27-33, 28-33, 37-33) and the production wells in section seven all received the tracer from the injection test well 25-5 (200 kg of 2-NS injected). The nearby injection wells in section 32 (wells 27-32, 38-32) could not be the source for the 2-NS tracer because these wells only inject cooling tower condensate and augmentation water which carry no recycled tracer (T. DeRocher, personal communication, 2007). The calculation of mass balance provides strong evidence for the source of this tracer flow. Tracer production from well 37-33 reached its peak on day 318 of the test, and on that day the cumulative production of 2-NS was 5.9 kg for well 37-33, 2.3 kg of tracer for well 27-33, and of 6.2 kg of tracer for well 28-33. It is clear that the slug tracer injection of 200 kg of 2-NS into well 25-5 and the cumulative tracer recycling of an additional

16 kg of 2-NS into well 25-5 were responsible for all of the cumulative 2-NS tracer production in section 33. Reservoir fluid flow from the section five injection wells to both sections seven and 33 (in opposite directions from section five) was demonstrated independently when water injection at rates up to 125 L/s into well 45-5 caused reservoir pressure increases of 6 kPa/day in idle well 45-33 and up to 19 kPa/day in producing well 74-7 (Benoit et al., 2000). The augmentation of fluid injection begun in July 1997 partially restored the reservoir pressure and reversed the reservoir fluid drawdown. It is possible that the addition of augmentation fluid also reestablished fluid pathways from the section five injection wells to the section 33 producing wells and may have reversed previous indications of a proposed barrier between the northeast and southwest producing areas in Dixie Valley.

Moment analysis of tracer tests from several injection-production well pairs in Dixie Valley (Table 1) provided mean residence times between 604 days and 1197 days for the tracer flow through the fractures connecting each well pair. Pore volumes between  $1.0 \cdot 10^7$  and  $3.5 \cdot 10^7$  m<sup>3</sup> were calculated for fracture volumes swept by the tracer tests at Dixie Valley. These volumes are about an order of magnitude larger than the fracture volume of  $2.04 \cdot 10^6$  m<sup>3</sup> swept by the tracer test at Beowawe geothermal field, and the mean residence times for tracer flow are much longer than 268.8 days for Beowawe (Shook, 2005).

Plots of the  $F-\Phi$  curves for the Dixie Valley wells show different levels of heterogeneity in the flow system between different injection-production well pairs. The data points of  $F-\Phi$  curves from a few of the well pairs (Table 1) range from high heterogeneity in the flow system where 10% of the fracture volume provides 40% or more of the fluid flow between injection well 41-18 and the section seven production wells (see Figure 8) to lower heterogeneity in the flow system where 10% of the fracture volume provides 24% of the fluid flow between the section 32 injection wells and the section 33 production wells. Reservoir fractures in Dixie Valley compare favorably to the more restricted fractures in the Beowawe reservoir where 60% of the fluid flow came from only 12% of the total fracture volume (Shook, 2005).

### CONCEPTUAL RESERVOIR MODEL

A more complete conceptual model of the Dixie Valley geothermal reservoir was developed as a result of the interpretation of tracer tests. From the results of tracer moment analysis, the Dixie Valley reservoir can be considered a set of sub-parallel fractures with narrow apertures (volumes up to  $3.5 \cdot 10^7$  m<sup>3</sup> contacted by the tracer flow), long mean

Table 1. Calculated Well-Pair Parameters from Tracer Moment Analysis

Injection / Production Wells	First Temporal Moment (days)	Pore Volume (m <sup>3</sup> )	F at $\Phi=10\%$	F at $\Phi=20\%$
I25-5 / P28-33	901	2.6E+07	33%	49%
I25-5 / P37-33	993	2.8E+07	35%	51%
I25-5 / P63-7	928	3.1E+07	34%	51%
I25-5 / P73-7	863	2.3E+07	24%	42%
I25-5 / P73B-7	932	3.3E+07	34%	51%
I25-5 / P74-7	1189	3.5E+07	31%	48%
I45-5 / P63-7	792	1.3E+07	31%	48%
I45-5 / P73-7	604	1.0E+07	27%	44%
I27-32 / P28-33	797	1.5E+07	24%	40%
I27-32 / P37-33	817	1.4E+07	24%	40%
I38-32 / P28-33	691	1.9E+07	24%	39%
I38-32 / P37-33	723	1.8E+07	24%	40%
I41-18 / P63-7	1193	1.3E+07	43%	58%
I41-18 / P74-7	1089	1.3E+07	42%	58%
I41-18 / P76A-7	983	1.2E+07	40%	57%
I65-18 / P76A-7	1197	1.7E+07	34%	49%

The spreadsheet calculations of tracer moment analysis are summarized for production wells that have a clear peak and later decline in tracer response. The first temporal moment (mean residence time) and the pore volume (fracture volume of tracer contact) characterize the fractures. The fraction of fluid flow,  $F$ , from both 10% and 20% of the storage capacity,  $\Phi$ , show the degree of reservoir heterogeneity.

residence times (up to 1197 days), and large surface areas (for high heat transfer) developed in the fault zone and adjacent damage zones that provide permeability. Tracer recovery from producing wells in the northeastern and southwestern areas of the Dixie Valley field show that both areas are receiving fluid flow from injection wells in the center of the field (section five), and there is no barrier to fluid flow in the Dixie Valley geothermal reservoir. The permeable zones provide conduits for fluid rising from depth and fluid flowing from injection to production wells. Antithetic sets of fractures provide permeable pathways for fluid injected into the Tertiary basalt zones to reach the main fractures. Based on the multiple tracer recovery peaks exhibited by some production wells, sets of several isolated fractures of different permeabilities and different lengths are thought to connect pairs of injection and production wells.

## ACKNOWLEDGEMENTS

This work was supported by the U. S. Department of Energy, Assistant Secretary for Energy Efficiency and Renewable Energy, through an interagency agreement with the U. S. Geological Survey. The author appreciates the access to proprietary well flow data kindly provided by T. DeRocher, Caithness Operating Company, LLC. P. E. Rose generously provided the tracer concentration data and insight into the testing. G. M. Shook and J. H. Forsmann helped greatly with explanations of the moment analysis spreadsheet and with reviews of this study. N. Davatzes and D. Moore kindly provided reviews of this manuscript.

## REFERENCES

- Benoit, D. (1992) "A Case History of Injection through 1991 at Dixie Valley, Nevada," *Geothermal Resources Council, Transactions*, **16**, 611-620.
- Benoit, D., Johnson S. and Kumataka M. (2000) "Development of an Injection Augmentation Program at the Dixie Valley, Nevada Geothermal Field" *Proceedings: World Geothermal Congress 2000, Kyushu – Tohoku, Japan*, 819-824.
- Desormier, W. L. (1987) "Dixie Valley Six Well Flow Test" *Geothermal Resources Council, Transactions*, **11**, 515-519.
- Reed, M. J. (1989) "Thermodynamic Calculations of Calcium Carbonate Scaling in Geothermal Wells, Dixie Valley Geothermal Field, U.S.A." *Geothermics*, **18**, 269-277.
- Rose, P. E., Benoit D., Lee S. G., Tandia B. and Kilbourn P. (2000) "Testing the Naphthalene Sulfonates as Geothermal Tracers at Dixie Valley, Ohaaki, and Awibengkok" *Stanford University, Proceedings, 25<sup>th</sup> Workshop on Geothermal Reservoir Engineering, Stanford, CA*, SGP-TR-165, 36-42.
- Rose, P. E., Johnson S. D., Kilbourn P. and Kasteler C. (2002) "Tracer Testing at Dixie Valley, Nevada, Using 1-Naphthalene Sulfonate and 2,6-Naphthalene Disulfonate" *Stanford University, Proceedings, 27<sup>th</sup> Workshop on Geothermal Reservoir Engineering, Stanford, CA*, SGP-TR-171, 308-313.
- Rose, P. E., Benoit W. R. and Kilbourn P. M. (2001) "The Application of the Polyaromatic Sulfonates as Tracers in Geothermal Reservoirs" *Geothermics*, **30**, 617-640.
- Shook, G. M. (2001) "Predicting Thermal Breakthrough in Heterogeneous Media from Tracer Tests" *Geothermics*, **30**, 573-589.

Shook, G. M. (2003) "A Simple Fast Method of Estimating Reservoir Geometry from Tracer Tests" *Geothermal Resources Council, Transactions*, **27**, 407-411.

Shook, G. M. (2005) "A Systematic Method for Tracer Test Analysis: An Example Using Beowawe Tracer Data" *Stanford University, Proceedings, 30<sup>th</sup> Workshop on Geothermal Reservoir Engineering, Stanford, CA*, SGP-TR-176, 56-61.

Shook, G. M. and Forsmann J. H. (2005) "Tracer Interpretation Using Temporal Moments on a Spreadsheet" *Idaho National Laboratory, Report INL/EXT-05-00400, Rev. 1*, 20 p.